

# ONIOM(DFT:MM) Study of 2-Hydroxyethylphosphonate Dioxygenase: What Determines the Destinies of Different Substrates?

Hajime Hirao<sup>\*,†</sup> and Keiji Morokuma<sup>\*,§</sup>

<sup>†</sup>Division of Chemistry and Biological Chemistry, School of Physical and Mathematical Sciences, Nanyang Technological University, 21 Nanyang Link, Singapore 637371, Singapore

<sup>§</sup>Fukui Institute for Fundamental Chemistry, Kyoto University, 34-4 Takano Nishihiraki-cho, Sakyo, Kyoto 606-8103, Japan

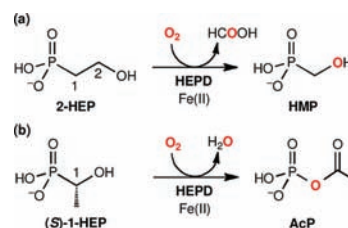
 Supporting Information

**ABSTRACT:** Why can enzymes provide different products from only slightly different substrates? While the reaction of 2-hydroxyethylphosphonate (2-HEP) catalyzed by 2-hydroxyethylphosphonate dioxygenase (HEPD) yields hydroxymethylphosphonate and formic acid, the HEPD-catalyzed reaction of 1-HEP gives acetylphosphate. ONIOM(DFT:MM) was used to uncover the distinct reaction mechanisms for the different substrates. Calculations show that, in both reactions, similar radical intermediates are generated by the same process. After the formation of common radical intermediates, proton-coupled electron transfer (PCET) operates in the 1-HEP reaction, whereas in the 2-HEP reaction, it cannot occur and an alternative pathway sets in. Thus, the PCET plays a critical role in defining the fates of the substrates.

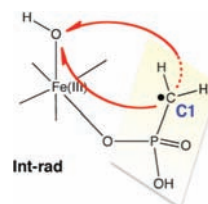
Iron enzymes having nonheme ligands are simply classified as nonheme iron enzymes, but evidence is growing that their reaction patterns are rather diverse. Some use ferric superoxide,<sup>1</sup> whereas others use ferryl (oxoiron(IV)) or ferric hydroperoxide to activate substrates.<sup>2</sup> Because these key intermediates are difficult to trap experimentally, the beneficial role of computational techniques, especially quantum mechanical and molecular mechanical (QM/MM) methods, is increasingly appreciated in discerning different reaction patterns of nonheme enzymes.<sup>3</sup>

Recently, nonheme enzymes that utilize ferric superoxide as a reactive species have become a topic of intense interest. Among such enzymes are 2-hydroxyethylphosphonate dioxygenase (HEPD),<sup>4</sup> *myo*-inositol oxygenase,<sup>3c,5</sup> isopenicillin N synthase,<sup>3a,b,6</sup> hydroxypropylphosphonic acid epoxidase,<sup>7</sup> and homoprotocatechuate 2,3-dioxygenase (2,3-HPCD).<sup>8</sup> HEPD is a particularly intriguing enzyme of this class, because it is involved in the biosynthesis of molecules containing a C–P bond, the so-called C–P compounds. C–P compounds are known to exhibit practically useful bioactivity as antibiotics, herbicides, and antimalarial compounds.<sup>9</sup> The recently solved X-ray structure of HEPD has shown that the enzyme is a mononuclear nonheme iron enzyme having a 2-His-carboxylate motif.<sup>4a</sup> For its catalytic reaction, HEPD utilizes Fe<sup>2+</sup> and O<sub>2</sub> and cleaves the C–C bond of 2-hydroxyethylphosphonate (2-HEP). The products of this reaction are hydroxymethylphosphonate (HMP) and formic acid (Scheme 1a). Very recently, Whitteck et al. introduced stereochemistry to the C1 of 2-HEP by replacing one of the two hydrogen atoms with deuterium, and demonstrated that the stereochemical information was lost after the enzymatic

Scheme 1. HEPD-Catalyzed Reactions



Scheme 2. Our Rationale for the Loss of Stereochemistry



reaction.<sup>4c</sup> This surprising finding was actually consistent with the mechanism proposed by us on the basis of density functional theory (DFT) calculations.<sup>4c</sup> The DFT calculations suggested that a substrate radical intermediate, designated here as **Int-rad** (Scheme 2), should be formed prior to product formation. The P–CH<sub>2</sub>· moiety of **Int-rad** can readily rotate about the P–C bond, and the attack of the CH<sub>2</sub>· moiety on the ferric-hydroxide unit can occur from either face of the molecular plane defined by P–CH<sub>2</sub>, thus, resulting in a loss of stereochemistry of the product at C1 (Scheme 2).

Another interesting feature of this enzyme is that different substrates appear to undergo different reactions. When 1-hydroxyethylphosphonate (1-HEP) is the substrate for the reaction (Scheme 1b), HEPD converts it to acetylphosphate (AcP).<sup>4b</sup> This finding means that, whereas HEPD acts as a dioxygenase in the 2-HEP reaction, in which the two oxygen atoms are incorporated into the formic acid and HMP products, it acts essentially as a monooxygenase in the 1-HEP reaction. In the latter, only one of the two oxygen atoms of O<sub>2</sub> is inserted into the substrate, and the other oxygen atom is converted to a water molecule (Scheme 1). What makes such a distinction? To answer this question, we have carried out extensive computational

Received: July 5, 2011

Published: August 29, 2011

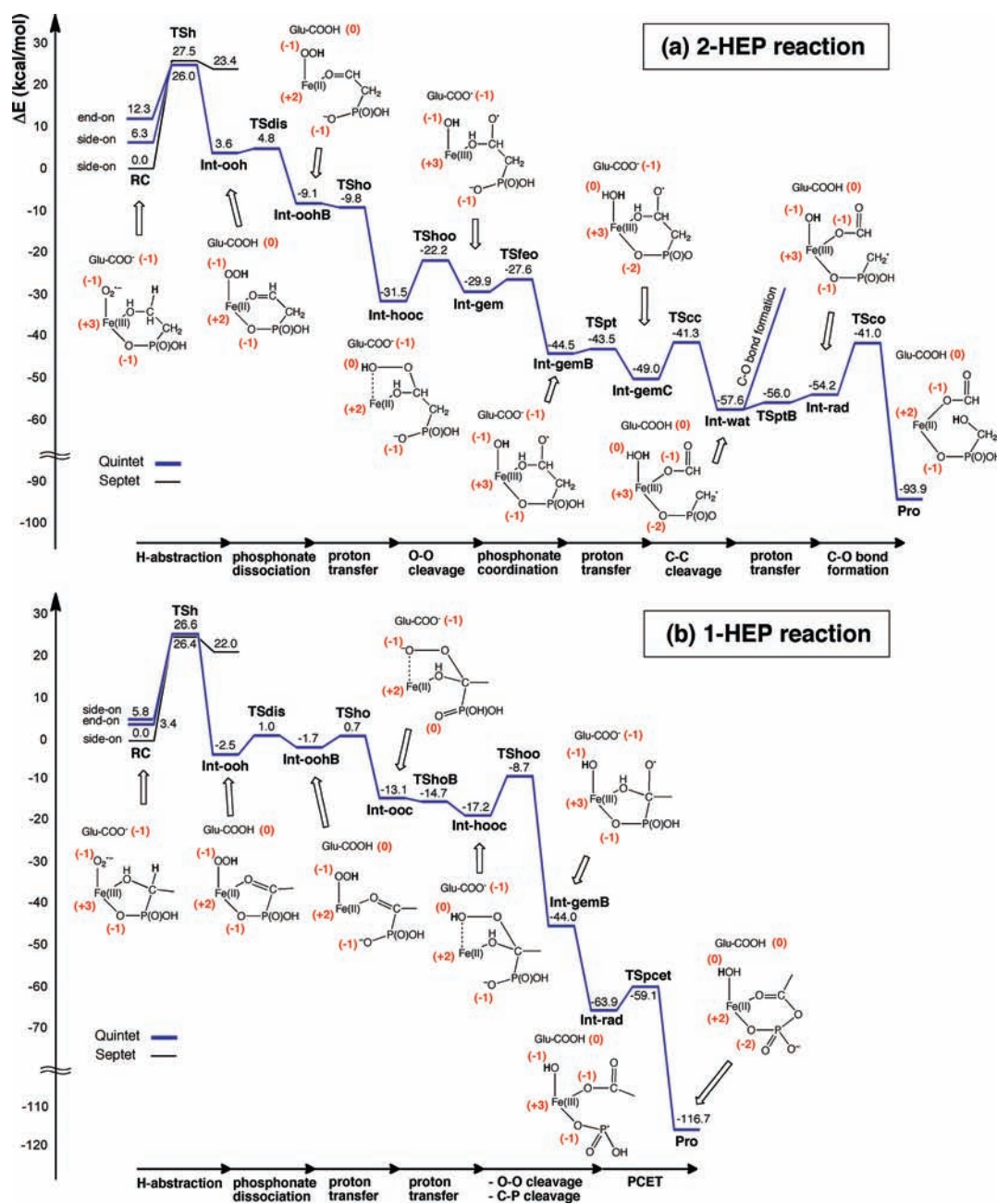


**Figure 1.** Energy profiles for the reactions of (a) 2-HEP and (b) 1-HEP, as obtained from ONIOM-EE(B3LYP/B2:AMBER)//ONIOM-EE(B3LYP/B1:AMBER)+ZPE. Formal group charges (in parentheses) are shown in red and the abstracted hydrogen is shown in boldface. Note that Glu above each structure denotes Glu176 that is coordinated to Fe using one of the carboxylate oxygen atoms.

studies using the ONIOM quantum mechanical (QM) and molecular mechanical (MM) method.<sup>10</sup>

Enzyme models of the ferric-superoxide intermediate of HEPD were constructed from an X-ray crystal structure (PDB code 3GBF, 1.92 Å resolution).<sup>4a</sup> As HEPD has a flexible protein structure, the residues within 8 Å from the iron center were optimized, while the other residues were kept frozen. The B3LYP functional<sup>11</sup> was used in conjunction with the SDD effective core potential basis set for Fe and the 6-31G\* basis set for the remaining atoms (basis set B1).<sup>12</sup> The 6-311+G(d,p) basis set (B2) was used for single-point energy calculations. Frequency calculations were performed with the outer atoms frozen as in the case of geometry optimization. These ONIOM(B3LYP:AMBER)<sup>13</sup>

electronic-embedding (ONIOM-EE) calculations were performed with Gaussian 09,<sup>14</sup> taking into account the polarization effect of the QM wave function in the presence of the surrounding amino acid residues. Further technical details, including the definition of the QM regions (Scheme S1), are given in the Supporting Information.

The reaction energy profile for 2-HEP is presented in Figure 1a. As shown by our previous DFT calculations,<sup>4c</sup> the initial step is the H-abstraction from C2 by a ferric-superoxide intermediate, which provides an Fe(II)OOH intermediate (**Int-ooH**). Although our calculations suggested that the septet state is the ground state for the reactant complex (**RC**), a recent experiment showed that the ferric-superoxide intermediate of 2,3-HPCD has

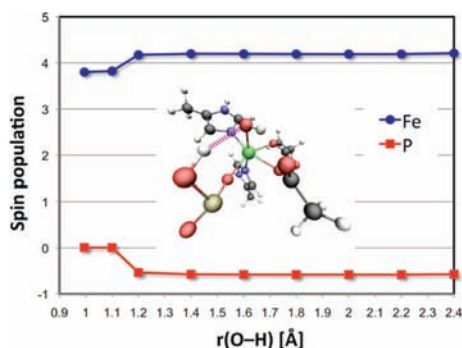
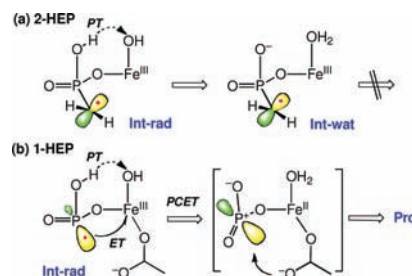


**Figure 2.** Change in the spin population on Fe and P in 1-HEP as a function of  $r(\text{O}-\text{H})$  (the reaction proceeds from right (**Int-rad**) to left (**Pro**)).

a quintet spin state, in which the high-spin ferric center is antiferromagnetically coupled to the superoxide unit.<sup>8</sup> Therefore, the septet state could be overstabilized using the DFT methods employed here. If we assume that the side-on quintet state is the ground state and the H-abstraction barrier is 19.7 kcal/mol, the kinetic isotope effect (KIE) at room temperature is calculated to be 5.7 and 8.0 with transition-state theory and its Wigner correction, respectively. These values are indirectly consistent with the observation that the HEPD-catalyzed oxidation of HMP exhibits a kinetic isotope effect of  $7.6 \pm 0.4$ .<sup>4c</sup> In the H-abstraction step, the proton of the hydroxyl group on C2 is donated to Glu176 to generate a carbonyl group (Figure 1). The Glu appears to accept the proton during the reaction stage where the C2–O bond is gaining double bond character. Because of the presence of surrounding H-bond donors, the phosphonate oxygen of **Int-ooH** was found to dissociate easily from the ferrous center, yielding **Int-ooH**. Subsequent proton transfer (PT), which is assisted by one of the phosphonate oxygen atoms, produces an R-OOH intermediate (**Int-hooc**). This somewhat complicated step was explained in great detail in our previous work.<sup>4e</sup> The O–O bond is then homolytically cleaved to yield a gem-diol radical intermediate (**Int-gem**). As this homolysis step changes the iron oxidation state back to +3, the phosphonate oxygen coordinates again to the iron. The resultant **Int-gemB** undergoes PT from phosphonate to Fe(III)OH to produce **Int-gemC**. Subsequently, the C–C bond between C1 and C2 is homolytically cleaved, and an intermediate (**Int-wat**) that contains a P–CH<sub>2</sub>·-type radical and formate is formed. C–O bond formation by attack of P–CH<sub>2</sub>· on the coordinating water was found to be unfavorable. However, if proton of the water ligand is back-donated to the phosphonate group and ferric hydroxide is formed (**Int-rad**), C–O bond formation is possible via **TScO**. The final product **Pro** contains HMP and formate. Whereas this C–O bond formation requires an energy barrier of 16.6 kcal/mol, the bond rotation of the P–CH<sub>2</sub>·-type radical should be easy. The observed loss of stereochemical information at C1 in **Pro** is thus attributed to this P–C bond rotation.

The reaction of 1-HEP (Figure 1b) is similar to that of 2-HEP up to **Int-gemB**, although a few minor differences can be seen. 1-HEP is not as flexible as 2-HEP, which prevents the phosphonate of 1-HEP from moving far from the Fe. Thus, the stabilization of the phosphonate by H-bonding is not as large as in 2-HEP. Indeed, **Int-ooH** is less stable in the 1-HEP reaction (Figure 1). After the O–O homolysis step in the 1-HEP reaction, the phosphonate oxygen spontaneously coordinated to the ferric

**Scheme 3.** PT of **Int-rad**: (a) 2-HEP; (b) 1-HEP



center. When the proton of the hydroxyl group at C1 of 1-HEP was transferred to the adjacent Glu176, the P–C bond of the substrate broke very easily, resulting in formation of acetate and ·PO<sub>2</sub>OH (**Int-rad**). The proton in the phosphonate OH group of the phosphite radical was then transferred with a low barrier to the hydroxide group of the ferric-hydroxide moiety. Interestingly, this PT is accompanied by electron transfer from the phosphorus radical center to Fe(III) when the proton moves to within 1.1 Å of the oxygen of the ferric hydroxide (Figure 2). At larger O–H distances, the Fe center possesses a spin population value of ~4.2, which is typical of the Fe(III) state, and the phosphorus center has some amount of spin population (~−0.57), which is indicative of radical character at P. At around 1.1 Å, however, these values change to ~3.8 and ~0.0, respectively, indicating that the iron is in the Fe(II) state and the phosphorus has lost radical character. This step is well described as proton-coupled electron transfer (PCET, see Scheme 3). This PCET gives the phosphorus center Lewis acid character, which in turn triggers nucleophilic attack of the acetate oxygen on the phosphorus. The combination of PCET and the nucleophilic attack finally provides an AcP complex (**Pro**). One may wonder if the attack of the phosphorus radical center in **Int-rad** of 1-HEP on the ferric-hydroxide can occur as in the 2-HEP reaction. However, this process was found to be unlikely.<sup>15</sup>

By contrast, PCET was not observed for the 2-HEP reaction, and PT of **Int-rad** just resulted in regenerating **Int-wat** (Figure 1; see also Scheme 3). The radical center present in **Int-rad** of 2-HEP is more distant from Fe than that of 1-HEP by one bond, which may be the reason why the electron transfer from the radical center to Fe does not take place efficiently.

In conclusion, our ONIOM studies revealed that the enzymatic reaction of HEPD involves radical intermediates. Different products are obtained for the reactions of 2-HEP and 1-HEP because of differences in the mechanism after the formation of common **Int-rad**. It is suggested that PCET renders monooxygenase activity to HEPD in the 1-HEP reaction.

## ■ ASSOCIATED CONTENT

Supporting Information. Complete ref 14, methodology, schematic illustrations of proposed mechanisms, raw energy data, and XYZ coordinates of QM atoms. This material is available free of charge via the Internet at <http://pubs.acs.org>.

## ■ AUTHOR INFORMATION

### Corresponding Authors

hirao@ntu.edu.sg; morokuma@fukui.kyoto-u.ac.jp



## ACKNOWLEDGMENT

The authors are grateful to Prof. W. A. van der Donk for providing unpublished data and very helpful discussions. H.H. thanks Nanyang Assistant Professorship for financial support and The High Performance Computing Centre at Nanyang Technological University for computer resources. This work was in part supported by a CREST grant in the Area of High Performance Computing for Multiscale and Multiphysics Phenomena from the Japan Science and Technology Agency (JST).

## REFERENCES

- (1) (a) Bollinger, J. M., Jr.; Krebs, C. *Curr. Opin. Chem. Biol.* **2007**, *11*, 151–158. (b) van der Donk, W. A.; Krebs, C.; Bollinger, J. M., Jr. *Curr. Opin. Struct. Biol.* **2010**, *20*, 673–683. (c) Emerson, J. P.; Farquhar, E. R.; Que, L., Jr. *Angew. Chem., Int. Ed.* **2007**, *46*, 8553–8556. (d) Joseph, C. A.; Maroney, M. J. *Chem. Commun.* **2007**, 3338–3349. (e) Kovaleva, E. G.; Lipscomb, J. D. *Nat. Chem. Biol.* **2008**, *4*, 186–193. (f) Buijninx, P. C. A.; van Koten, G.; Klein Gebbink, R. J. M. *Chem. Soc. Rev.* **2008**, *37*, 2716–2744. (g) Mukherjee, A.; Cranswick, M. A.; Chakrabarti, M.; Paine, T. K.; Fujisawa, K.; Münck, E.; Que, L., Jr. *Inorg. Chem.* **2010**, *49*, 3618–3628.
- (2) (a) Ye, S.; Neese, F. *Curr. Opin. Chem. Biol.* **2009**, *13*, 89–98. (b) Pau, M. Y. M.; Lipscomb, J. D.; Solomon, E. I. *Proc. Nat. Acad. Sci. U.S.A.* **2007**, *104*, 18355–18362. (c) Solomon, E. I.; Wong, S. D.; Liu, L. V.; Decker, A.; Chow, M. S. *Curr. Opin. Chem. Biol.* **2009**, *13*, 99–113.
- (3) (a) Lundberg, M.; Morokuma, K. *J. Phys. Chem. B* **2007**, *111*, 9380–9389. (b) Lundberg, M.; Kawatsu, T.; Vreven, T.; Frisch, M. J.; Morokuma, K. *J. Chem. Theory Comput.* **2009**, *5*, 222–234. (c) Hirao, H.; Morokuma, K. *J. Am. Chem. Soc.* **2009**, *131*, 17206–17214. (d) Kumar, D.; Thiel, W.; de Visser, S. P. *J. Am. Chem. Soc.* **2011**, *133*, 3869–3882.
- (4) (a) Cicchillo, R. M.; Zhang, H.; Blodgett, J. A. V.; Whitteck, J. T.; Li, G.; Nair, S. K.; van der Donk, W. A.; Metcalf, W. W. *Nature* **2009**, *459*, 871–874. (b) Whitteck, J. T.; Cicchillo, R. M.; van der Donk, W. A. *J. Am. Chem. Soc.* **2009**, *131*, 16225–16232. (c) Whitteck, J. T.; Malova, P.; Peck, S. C.; Cicchillo, R. M.; Hammerschmidt, F.; van der Donk, W. A. *J. Am. Chem. Soc.* **2011**, *133*, 4236–4239. (d) Peck, S. C.; Cooke, H. A.; Cicchillo, R. M.; Malova, P.; Hammerschmidt, F.; Nair, S. K.; van der Donk, W. A. *Biochemistry* **2011**, *50*, 6598–6605. (e) Hirao, H.; Morokuma, K. *J. Am. Chem. Soc.* **2010**, *132*, 17901–17909.
- (5) (a) Bollinger, J. M., Jr.; Diao, Y.; Matthews, M. L.; Xing, G.; Krebs, C. *Dalton Trans.* **2009**, 905–914. (b) Xing, G.; Diao, Y.; Hoffart, L. M.; Barr, E. W.; Prabhu, K. S.; Arner, R. J.; Reddy, C. C.; Krebs, C.; Bollinger, J. M., Jr. *Proc. Natl. Acad. Sci. U.S.A.* **2006**, *103*, 6130–6135. (c) Brown, P. M.; Caradoc-Davies, T. T.; Dickson, J. M. J.; Cooper, G. J. S.; Loomes, K. M.; Baker, E. N. *Proc. Natl. Acad. Sci. U.S.A.* **2006**, *103*, 15032–15037.
- (6) (a) Roach, P. L.; Clifton, I. J.; Hensgens, C. M. H.; Shibata, N.; Schofield, C. J.; Baldwin, J. E. *Nature* **1997**, *387*, 827–830. (b) Brown, C. D.; Neidig, M. L.; Neibergall, M. B.; Lipscomb, J. D.; Solomon, E. I. *J. Am. Chem. Soc.* **2007**, *129*, 7427–7438. (c) Lundberg, M.; Siegbahn, P. E. M.; Morokuma, K. *Biochemistry* **2008**, *47*, 1031–1042.
- (7) Yun, D.; Dey, M.; Higgins, L. J.; Yan, F.; Liu, H-w.; Drennan, C. L. *J. Am. Chem. Soc.* **2011**, *133*, 11262–11269.
- (8) Mbughuni, M. M.; Chakrabarti, M.; Hayden, J. A.; Bominaar, E. L.; Hendrich, M. P.; Munck, E.; Lipscomb, J. D. *Proc. Nat. Acad. Sci. U.S.A.* **2010**, *107*, 16788–16793.
- (9) Metcalf, W. W.; van der Donk, W. A. *Annu. Rev. Biochem.* **2009**, *78*, 65–94.
- (10) Vreven, T.; Byun, K. S.; Komáromi, I.; Dapprich, S.; Montgomery, J. A., Jr.; Morokuma, K.; Frisch, M. J. *J. Chem. Theory Comput.* **2006**, *2*, 815–826.
- (11) (a) Becke, A. D. *J. Chem. Phys.* **1993**, *98*, 5648–5652. (b) Lee, C.; Yang, W.; Parr, R. G. *Phys. Rev. B* **1988**, *37*, 785–789. (c) Vosko, S. H.; Wilk, L.; Nusair, M. *Can. J. Phys.* **1980**, *58*, 1200–1211.
- (12) (a) Dolg, M.; Wedig, U.; Stoll, H.; Preuss, H. *J. Chem. Phys.* **1987**, *86*, 866–872. (b) Hehre, W.; Radom, L.; Schleyer, P.; Pople, J. *Ab Initio Molecular Orbital Theory*; John Wiley & Sons: New York, 1986.
- (13) Cornell, W. D.; Cieplak, P.; Bayly, C. I.; Gould, I. R.; Merz, K. M., Jr.; Ferguson, D. M.; Spellmeyer, D. C.; Fox, T.; Caldwell, J. W.; Kollman, P. A. *J. Am. Chem. Soc.* **1995**, *117*, 5179–5197.
- (14) *Gaussian 09*, revision B.01; Frisch, M. J.; et al. Gaussian, Inc.: Wallingford, CT, 2010.
- (15) PCET (Figure 2) occurred during the scan calculation using the P–O distance as the reaction coordinate, thus converging to **Pro**.